Gyroscopic Stabilization of Unstable Vehicles: Configurations, Dynamics, and Control

Stephen C. Spry* and Anouck R. Girard†

March 31, 2008

Abstract

We consider active gyroscopic stabilization of unstable bodies such as two-wheeled monorails, two-wheeled cars, or unmanned bicycles. It has been speculated that gyroscopically stabilized monorail cars would have economic advantages with respect to birail cars, enabling the cars to take sharper curves and traverse steeper terrain, with lower installation and maintenance costs. A two-wheeled, gyro-stabilized car was actually constructed in 1913.

The dynamic stabilization of a monorail car or two-wheeled automobile requires that a torque acting on the car from the outside be neutralized by a torque produced within the car by a gyroscope. The gyroscope here is used as an actuator, not a sensor, by using precession forces generated by the gyroscope. When torque is applied to an axis normal to the spin axis, causing the gyroscope to precess, a moment is produced about a third axis, orthogonal to both the torque and spin axes. As the vehicle tilts from vertical, a precession-inducing torque is applied to the gyroscope cage such that the resulting gyroscopic reaction moment will tend to right the vehicle. The key idea is that motion of the gyroscope relative to the body is actively controlled in order to generate a stabilizing moment.

This problem was considered in 1905 by Louis Brennan [1]. Many extensions were later developed, including the work by Shilovskii [2], and several prototypes were built. The differences in the various schemes lie in the number of gyroscopes employed, the direction of the spin axes relative to the rail, and in the method used to produce precession of the spin axes.

We start by deriving the equations of motion for a case where the system is formed of a vehicle, a load placed on the vehicle, the gyroscope wheel, and a gyroscope cage. We allow for track curvature and vehicle speed. We then derive the equations for a similar system with two gyroscopes, spinning in opposite directions and such that the precession angles are opposite. We linearize the dynamics about a set of equilibrium points and develop a linearized model. We study the stability of the linearized systems and show simulation results. Finally, we discuss a scaled gyrovehicle model and testing.

Index Terms- Gyroscopic stabilization, monorails

1 INTRODUCTION

The single track gyroscopic vehicle problem is first considered in 1905 by Louis Brennan [1]. Many extensions were later developed, including the work by Shilovskii [2, 4], and several prototypes were built [3]. The differences in the various schemes lie in the number of gyroscopes employed, the direction of the spin axles relative to the rail, and in the method used to produce the acceleration of the spin axle. The online Museum of Retro Technology [7] cites many articles and examples of gyrocars, including a 1961 Ford Gyrocar concept called the Gyron and a concept from Gyro Transport Systems of Northridge, California that was on the cover of the September, 1967 issue of "Science and Mechanics". Other important application of gyroscopic stabilizers include to ships and ocean vehicles, as discussed in [5, 6], and robotics [8, 9, 10].

Mathematical analysis of the two-wheeled vehicle gyroscopic stabilization problem first appears in [14], and more recently in [12], without derivation, or in [13], where the derivation is by use of bond graphs. The

---

*S.C. Spry is with Lam Research Corporation, Fremont, CA 94538 (email: stephen.spry@lamrc.com).

†A. R. Girard is with the Department of Aerospace Engineering, University of Michigan, Ann Arbor, MI 48109. (email: anouck@umich.edu).

problem also appears as a homework problem in [15]. A possible controller for stationary regimes is proposed in [11].

Our work is different in that we derive the equations of motion using Lagrangian mechanics, and in that we study several configurations, and propose linear controllers and stability analysis for the system based on the derived model.

The control problem is to roll-stabilize an unstable cart. In the cart design, destabilizing forces are resisted by a gyroscope, which is driven by a motor. The gyroscope here is used as an actuator, not a sensor, by using precession forces generated by the gyroscope. When torque is applied to an axis normal to the spin axis, the gyroscope reacts by producing a reaction moment about a third axis, orthogonal to both the torque and spin axes [2].

The paper is organized as follows. In section II, we start by developing dynamic equations for a gyroscopically stabilized cart. We model the nonlinear dynamics of the cart and gyroscope using Lagrange's method. We study different configurations, including the single and double gyroscope cases. In section III, we develop a linearized model, and perform stability analysis of the closed-loop feedback system. The control problem is to roll-stabilize the cart. In section IV, we show simulation results. Finally, we discuss a scaled model that was built in section V.

2   EQUATIONS OF MOTION

We begin by defining terms and quantities to be used in the derivation (See Figures 1 and 2):

- B, L, C, and G refer to the body of the vehicle, a load placed on the vehicle, the gyro cage, and the gyro wheel respectively. These letters will also refer to frames fixed within those bodies.

- b, l, c, and g are points at the mass centers of bodies B, L, C, and G respectively.

- m and I, with subscripts B, L, C, or G denote the mass and moments of inertia of the corresponding body.

- ϕ is the roll angle of the vehicle.

- α is the precession angle of the gyroscope.

- s is the point on the track at the midpoint of the track segment defined by the contact points of the front and rear wheels of the vehicle. $\dot{s}$ is the speed of this point.

- $\dot{\psi}$ is the vertical component of vehicle rotation. This is determined by vehicle speed and track curvature.

- r is the track radius of curvature.

- h is the distance from the midpoint of the wheelbase line (the line segment between the contact points of the front and rear wheels) to the track. This is a function of wheelbase and radius of curvature: $h = r - (1/2)\sqrt{4r^2 - d_w^2}$, where d_w is the wheelbase. $h = 0$ for straight track.

- σ is the speed of the midpoint of the wheelbase line. For finite r ($h > 0$), σ is related to $\dot{s}$ and $\dot{\psi}$ by $\sigma = \dot{s}(r - h)/r = \dot{\psi}(r - h)$. For straight track ($h = 0$), $\sigma = \dot{s}$.

- d_1, d_2, and d_l are the distances from the wheelbase line to the mass centers of the body, the gyro wheel, and the load respectively.

- x_l, y_l, and z_l are the coordinates (in frame B) of point l relative to the midpoint of the wheelbase line.

- ϕ_l is the angle between $\mathbf{b}_3$ and point l.

- F_d is a horizontal disturbance force acting on the vehicle, applied at point b.

We define the following right-handed reference frames:
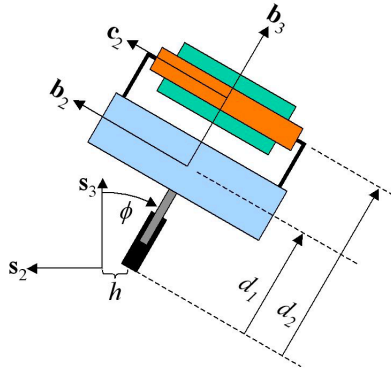
Figure 1: Gyroscopically stabilized cart - back view schematic
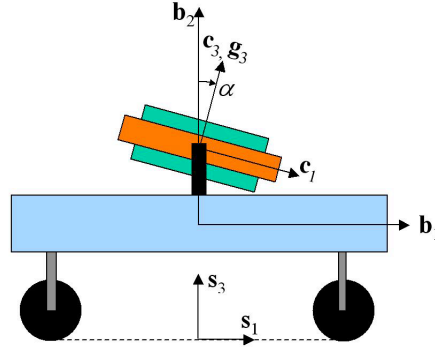
Figure 2: Gyroscopically stabilized cart - side view schematic

- A is earth-fixed, with $\mathbf{a}_3$ pointing upward, opposite to the gravity vector.

- S moves along the track with the vehicle. At point s, $\mathbf{s}_1$ is tangent to the track, $\mathbf{s}_2$ is normal, and $\mathbf{s}_3$ is binormal. For motion on a horizontal track, frame S rotates about $\mathbf{s}_3$ at a rate of $\dot{\psi}$.

- B is fixed in the body of the vehicle, with $\mathbf{b}_1$ pointing forward, $\mathbf{b}_2$ pointing left, and $\mathbf{b}_3$ pointing upward. $\mathbf{b}_1$ is always aligned with $\mathbf{s}_1$, and frame B is aligned with frame S when $\phi = 0$.

- C is attached to the gyro cage such that $\mathbf{c}_2$ is always aligned with $\mathbf{b}_2$, and frame C is aligned with frame B when $\alpha = 0$.

- G is attached to the gyro wheel such that $\mathbf{g}_3$ is always aligned with $\mathbf{c}_3$ and frame G is aligned with frame C once per rotation of the gyro wheel.

Single Gyro System

We now develop the equations of motion for the system using Lagrangian mechanics. In the equations, we follow standard practice notation and abbreviate "sin" with "s" and "cos" with "c". We start by considering motion along a horizontal track.

Velocity expressions are:

$$^{A}\boldsymbol{\omega}^{B} = {}^{A}\boldsymbol{\omega}^{L} = \omega_1 \mathbf{b}_1 + \omega_2 \mathbf{b}_2 + \omega_3 \mathbf{b}_3 \tag{1}$$

$$^A\boldsymbol{\omega}^C = \omega_4\mathbf{c}_1 + \omega_5\mathbf{c}_2 + \omega_6\mathbf{c}_3 \tag{2}$$

$$^A\boldsymbol{\omega}^G = {}^A\boldsymbol{\omega}^C + \Omega\mathbf{c}_3 \tag{3}$$

$$^A\mathbf{v}^b = v_1\mathbf{b}_1 - v_2\mathbf{b}_2 \tag{4}$$

$$^A\mathbf{v}^g = v_3\mathbf{b}_1 - v_4\mathbf{b}_2 \tag{5}$$

$$^A\mathbf{v}^l = v_5\mathbf{b}_1 + v_6\mathbf{b}_2 + v_7\mathbf{b}_3 \tag{6}$$

where

$$
\begin{aligned}
\omega_1 &= \dot{\phi}\\
\omega_2 &= \dot{\psi}s\phi\\
\omega_3 &= \dot{\psi}c\phi\\
\omega_4 &= \dot{\phi}c\alpha - \dot{\psi}c\phi s\alpha\\
\omega_5 &= \dot{\psi}s\phi + \dot{\alpha}\\
\omega_6 &= \dot{\phi}s\alpha + \dot{\psi}c\phi c\alpha
\end{aligned}
$$

and

$$
\begin{aligned}
v_1 &= \sigma + \omega_2 d_1\\
v_2 &= \omega_1 d_1\\
v_3 &= \sigma + \omega_2 d_2\\
v_4 &= \omega_1 d_2\\
v_5 &= \sigma + \omega_2 z_l - \omega_3 y_l\\
v_6 &= \omega_3 x_l - \omega_1 z_l\\
v_7 &= \omega_1 y_l - \omega_2 x_l
\end{aligned}
$$

Kinetic energy expressions are:

$$T_B = \frac{1}{2}m_B(v_1^2 + v_2^2) + \frac{1}{2}(\omega_1^2 I_{B11} + \omega_2^2 I_{B22} + \omega_3^2 I_{B33}) \tag{7}$$

$$T_L = \frac{1}{2}m_L(v_5^2 + v_6^2 + v_7^2) + \frac{1}{2}(\omega_1^2 I_{L11} + \omega_2^2 I_{L22} + \omega_3^2 I_{L33}) \tag{8}$$

$$T_C = \frac{1}{2}m_C(v_3^2 + v_4^2) + \frac{1}{2}(\omega_4^2 I_{C11} + \omega_5^2 I_{C22} + \omega_6^2 I_{C33}) \tag{9}$$

$$T_G = \frac{1}{2}m_G(v_3^2 + v_4^2) + \frac{1}{2}(\omega_4^2 I_{G11} + \omega_5^2 I_{G22} + (\omega_6 + \Omega)^2 I_{G33}) \tag{10}$$

The total kinetic energy of the system is

$$T = T_B + T_L + T_C + T_G \tag{11}$$

We now apply Lagrange's equations in the form

$$\frac{d}{dt}\left(\frac{\partial T}{\partial \dot{q}_i}\right) - \frac{\partial T}{\partial q_i} = Q_i \tag{12}$$

where the q_i and Q_i are generalized coordinates and forces for the system.

This leads to the following equations for ϕ and α:

$$\ddot{\phi}(k_9 + c^2\alpha k_4 + s^2\alpha k_6) - 2\dot{\phi}\dot{\alpha}s\alpha c\alpha k_{10}$$

$$+\dot{\psi}\dot{\alpha}c\phi((s^2\alpha - c^2\alpha)k_{10} - k_5)$$

$$-\sigma\dot{\psi}((c\phi z_l + s\phi y_l)m_L + c\phi k_7)$$
$$-\dot{\psi}^2 c\phi s\phi(k_8 + k_2 - k_3 + k_5 - s^2\alpha k_4 - c^2\alpha k_6)$$
$$-\dot{\psi}^2 m_L(c\phi s\phi(z_l^2 - y_l^2) + (s^2\phi - c^2\phi)z_l y_l)$$
$$+\dot{\alpha}c\alpha\Omega I_{G33} + \dot{\psi}c\alpha s\phi\Omega I_{G33} = \tag{13}$$
$$k_7 gs\phi + m_L d_l gs(\phi + \phi_l) + F_a d_1 c\phi$$

$$\ddot{\alpha}k_5 + \dot{\psi}\dot{\phi}c\phi k_5$$
$$+(\dot{\phi}^2 c\alpha s\alpha - \dot{\psi}^2 c^2\phi c\alpha s\alpha - \dot{\psi}\dot{\phi}c\phi(s^2\alpha - c^2\alpha))k_{10}$$
$$+\Omega(\dot{\psi}c\phi s\alpha - \dot{\phi}c\alpha)I_{G33} = M_u \tag{14}$$

where

$$
\begin{aligned}
k_1 &= I_{B11} + I_{L11} \\
k_2 &= I_{B22} + I_{L22} \\
k_3 &= I_{B33} + I_{L33} \\
k_4 &= I_{C11} + I_{G11} \\
k_5 &= I_{C22} + I_{G22} \\
k_6 &= I_{C33} + I_{G33} \\
k_7 &= d_1 m_B + d_2(m_C + m_G) \\
k_8 &= d_1^2 m_B + d_2^2(m_C + m_G) \\
k_9 &= k_1 + k_8 + (y_l^2 + z_l^2)m_L \\
k_{10} &= k_4 - k_6
\end{aligned}
$$

Double Gyro System

We now consider the addition of a second gyro to the vehicle. We assume that this second gyro spins in the opposite direction to the first and that it is linked to the first gyro such that the precession angles are opposite:

$$\Omega_2 = -\Omega$$

$$\alpha_2 = -\alpha$$

To keep the total gyroscopic momentum the same, each of the two gyros and cages will have mass properties that are half those of the corresponding single gyro components. For simplicity, we assume that, for the gyros and cages, the mass centers are collocated and the precession axes are the same. With these asssumptions, the velocity expressions for the second gyro are:

$$^A\boldsymbol{\omega}^{C2} = \omega_7 \mathbf{c}_{21} + \omega_8 \mathbf{c}_{22} + \omega_9 \mathbf{c}_{23} \tag{15}$$

$$^A\boldsymbol{\omega}^{G2} = {}^A\boldsymbol{\omega}^{C2} - \Omega\mathbf{c}_{23} \tag{16}$$

$$^A\mathbf{v}^{c2} = {}^A\mathbf{v}^{g2} = {}^A\mathbf{v}^c = {}^A\mathbf{v}^g \tag{17}$$

where

$$
\begin{aligned}
\omega_7 &= \dot{\phi}c\alpha + \dot{\psi}c\phi s\alpha \\
\omega_8 &= \dot{\psi}s\phi - \dot{\alpha} \\
\omega_9 &= -\dot{\phi}s\alpha + \dot{\psi}c\phi c\alpha
\end{aligned}
$$

The kinetic energies are:

$$T_{C2} = \frac{1}{2}(\frac{1}{2}m_C(v_3^2 + v_4^2) + \frac{1}{2}(\omega_7^2 I_{C11} + \omega_8^2 I_{C22} + \omega_9^2 I_{C33})) \tag{18}$$

$$T_{G2} = \frac{1}{2}(\frac{1}{2}m_G(v_3^2 + v_4^2) + \frac{1}{2}(\omega_7^2 I_{G11} + \omega_8^2 I_{G22} + (\omega_9 - \Omega)^2 I_{G33})) \tag{19}$$

The total kinetic energy of the double gyro system is

$$T = T_B + T_L + (T_C + T_G)/2 + T_{C2} + T_{G2} \tag{20}$$

This leads to the following equations for ϕ and α:

$$\ddot{\phi}(k_9 + (c^2\alpha k_4 + s^2\alpha k_6)) - 2\dot{\phi}\dot{\alpha}s\alpha c\alpha k_{10}$$

$$-\dot{\psi}\sigma(k_7 c\phi + (z_l c\phi + y_l s\phi)m_L)$$

$$-\dot{\psi}^2 c\phi s\phi(k_8 + k_2 - k_3 + k_5 - s^2\alpha k_4 - c^2\alpha k_6)$$

$$-\dot{\psi}^2 m_L(c\phi s\phi(z_l^2 - y_l^2) + (s^2\phi - c^2\phi)z_l y_l)$$

$$+\dot{\alpha}c\alpha\Omega I_{G33}$$

$$= k_7 gs\phi + m_L d_l gs(\phi + \phi_l) + F_d d_1 c\phi \tag{21}$$

$$\ddot{\alpha}k_5 + (\dot{\phi}^2 c\alpha s\alpha - \dot{\psi}^2 c^2\phi c\alpha s\alpha)k_{10} - \dot{\phi}c\alpha\Omega I_{G33} = M_u \tag{22}$$

Inclined Track

The dynamical equations for motion on a straight inclined track can be easily obtained from the equations above by:

i.) Setting $\dot{\psi} = 0$. S does not rotate with respect to A in this case.

ii.) Replacing g with $gc\gamma$ in the expression for the generalized force Q_ϕ, so that

$$Q_\phi = k_7 gc\gamma s\phi + m_L d_l gc\gamma s(\phi + \phi_l) + F_d d_1 c\phi$$

where γ is the incline angle.

3   Linear Approximation and Analysis

In order to gain some understanding of the basic characteristics of the system, we now consider behavior of the system in the neighborhood of its equilibrium points. We define the state vector $\mathbf{x} = (\phi, \alpha, \dot{\phi}, \dot{\alpha})$.

Single Gyro System

We assume that $\dot{\psi}$ is small and that m_L and F_d are zero, and then linearize about $\mathbf{x} = 0$ to obtain the approximate dynamical equations for ϕ and α:

$$\ddot{\phi}(k_9 + k_4) - \sigma\dot{\psi}k_7 + \dot{\alpha}\Omega I_{G33} + \dot{\psi}\phi\Omega I_{G33} = k_7 g\phi$$

$$\ddot{\alpha}k_5 + \Omega(\dot{\psi}\alpha - \dot{\phi})I_{G33} = M_u \tag{23}$$

Defining a contol input

$$M_u = -K_\alpha\alpha - C_\alpha\dot{\alpha} + K_\phi\phi + M_2$$

we write state equations in the standard form $\dot{\mathbf{x}} = \mathbf{f}(\mathbf{x})$, where

$$\mathbf{f}(\mathbf{x}) = \begin{bmatrix} \dot{\phi} \\ \dot{\alpha} \\ \frac{1}{(k_9+k_4)}(k_7 g\phi - \dot{\alpha}\Omega I_{G33} - \dot{\psi}(\phi\Omega I_{G33} - \sigma k_7)) \\ \frac{1}{k_5}(\Omega I_{G33}\dot{\phi} - \dot{\psi}\Omega I_{G33}\alpha - K_\alpha\alpha - C_\alpha\dot{\alpha} + K_\phi\phi + M_2) \end{bmatrix} \tag{24}$$

Setting $\mathbf{f}(\mathbf{x}) = 0$, the equilibrium values of ϕ and α (with $M_2 = 0$) are found to be:

$$\phi_n = -\frac{\dot{\psi}\sigma k_7}{k_7 g - \dot{\psi}\Omega I_{G33}}$$ (25)

and

$$\alpha_n = \phi_n \frac{K_\phi}{K_\alpha + \dot{\psi}\Omega I_{G33}}$$ (26)

Writing the state equations in matrix form gives

$$\dot{\mathbf{x}} = \begin{bmatrix} 0 & 0 & 1 & 0 \\ 0 & 0 & 0 & 1 \\ a & 0 & 0 & b \\ f & c & d & e \end{bmatrix} \mathbf{x} + \begin{bmatrix} 0 \\ 0 \\ \dot{\psi}\sigma k_7/(k_9 + k_4) \\ M_2/k_5 \end{bmatrix}$$ (27)

where

$$a = \frac{1}{(k_9 + k_4)}(k_7 g - \dot{\psi}\Omega I_{G33})$$

$$b = \frac{-\Omega I_{G33}}{(k_9 + k_4)}$$

$$c = \frac{1}{k_5}(-K_\alpha - \dot{\psi}\Omega I_{G33})$$

$$d = \frac{\Omega I_{G33}}{k_5}$$

$$e = \frac{-C_\alpha}{k_5}$$

$$f = \frac{K_\phi}{k_5}$$

A necessary condition for stability of the system (27) is that all coefficients of the characteristic equation

$$det(sI - A) = s^4 - es^3 - (db + c + a)s^2 + (ae - bf)s + ac = 0$$ (28)

be positive.

The resulting conditions on the coefficients of the characteristic equation lead to the following conditions on system parameters $\dot{\psi}$, Ω, K_ϕ, C_α, and K_α (we assume $\Omega > 0$):

- $e < 0$:
$$C_\alpha > 0$$ (29)

- $db + c + a < 0$:
$$K_\alpha > \frac{k_5 k_7 g - (\Omega I_{G33})^2 - (k_9 + k_4 + k_5)\Omega I_{G33}\dot{\psi}}{(k_9 + k_4)}$$ (30)

- $ac > 0$:
$$\dot{\psi}\Omega I_{G33} < \min(-K_\alpha, k_7 g)$$ (31)

Note that for $\dot{\psi} = 0$, this requires $K_\alpha < 0$.

- $ae - bf > 0$:
$$K_\phi > \frac{C_\alpha(k_7 g - \dot{\psi}\Omega I_{G33})}{\Omega I_{G33}}$$ (32)

Double Gyro System

As in the single gyro case, we assume that $\dot{\psi}$ is small and that m_L and F_d are zero, and then linearize about $\mathbf{x} = 0$. This leads to the following approximate equations for ϕ and α:

$$\ddot{\phi}(k_9 + k_4) - \sigma\dot{\psi}k_7 + \dot{\alpha}\Omega I_{G33} = k_7 g\phi$$

$$\ddot{\alpha}k_5 - \dot{\phi}\Omega I_{G33} = M_u \tag{33}$$

The state equations are $\dot{\mathbf{x}} = \mathbf{f}(\mathbf{x})$, where:

$$\mathbf{f}(\mathbf{x}) = \begin{bmatrix} \dot{\phi} \\ \dot{\alpha} \\ \frac{1}{(k_9+k_4)}(k_7 g\phi - \dot{\alpha}\Omega I_{G33} + \dot{\psi}\sigma k_7) \\ \frac{1}{k_5}(\Omega I_{G33}\dot{\phi} - K_\alpha\alpha - C_\alpha\dot{\alpha} + K_\phi\phi + M_2) \end{bmatrix} \tag{34}$$

The equilibrium values of ϕ and α are found to be:

$$\phi_n = -\frac{\dot{\psi}\sigma}{g} \tag{35}$$

and

$$\alpha_n = \phi_n\frac{K_\phi}{K_\alpha} \tag{36}$$

The double gyro state equations take exactly the same form as (27), with the matrix elements now defined as:

$$a = \frac{k_7 g}{(k_9 + k_4)}$$

$$b = \frac{-\Omega I_{G33}}{(k_9 + k_4)}$$

$$c = \frac{-K_\alpha}{k_5}$$

$$d = \frac{\Omega I_{G33}}{k_5}$$

$$e = \frac{-C_\alpha}{k_5}$$

$$f = \frac{K_\phi}{k_5}$$

Unlike the single gyro case, none of the matrix elements for the double gyro system are dependent on $\dot{\psi}$.

The stability conditions on system parameters for the double gyro system are:

- $e < 0$:

$$C_\alpha > 0 \tag{37}$$

- $db + c + a < 0$:

$$K_\alpha > \frac{k_5 k_7 g - (\Omega I_{G33})^2}{(k_9 + k_4)} \tag{38}$$

- $ac > 0$:

$$K_\alpha < 0 \tag{39}$$

- $ae - bf > 0$:

$$K_\phi > \frac{C_\alpha k_7 g}{\Omega I_{G33}} \tag{40}$$

These conditions are simpler than those for the single gyro system. Most significantly, they do not depend on turn rate; in fact, they are the same as the single gyro conditions for zero turn rate.

4   SIMULATIONS

In this section, we present simulation results for a model-size gyrovehicle. Parameters are chosen to correspond to the experimental vehicle described in the next section. Simulations of the different gyroscope configurations were run using Matlab. The full nonlinear dynamics were simulated, along with the linear feedback controller designed in Section 3.

A number of simulations were performed to verify the stability conditions established in Section 3 for the single gyroscope case. For the sake of simplicity, the plots shown are for the case where the turn rate, $\dot{\psi}$, is equal to zero. Figures 3, 4, and 5 illustrate some of the different conditions. In those figures, two of the controller gains are chosen to meet the stability conditions, while the third is allowed to vary, to illustrate the transition from stability to instability. The plots show the angle of the gyroscope and the angle of the vehicle/cart; the desired behavior is for both those angles to converge to zero. In each figure, initial conditions for α and ϕ are $\alpha = 25\,\mathrm{deg}$ and $\phi = 2\,\mathrm{deg}$.

In Figure 3, C_α and K_ϕ are chosen to meet stability conditions, while K_α is allowed to be strictly positive (unstable), zero (unstable), or strictly negative (stable). The plot, which shows typical behavior for positive, zero, and negative values of K_α, illustrates that stable behavior does require $K_\alpha < 0$.

In Figure 4, K_α and K_ϕ are chosen to meet stability conditions, while C_α is allowed to be strictly positive (stable), zero (unstable), or strictly negative (unstable). This plot validates the condition on C_α, showing that $C_\alpha > 0$ is required for stable behavior.

Similarly, in Figure 5, K_α and C_α are chosen to meet stability conditions, while K_ϕ is allowed to be twice the required constant (stable), exactly equal to the constant (unstable), or half the value of the constant (unstable). Satisfaction of the condition on K_ϕ is shown to be necessary for stability.

Simulations were then performed to illustrate the dependency on the turn rate and direction, $\dot{\psi}$, for the single gyroscope case as opposed to the double gyroscope case. For a given set of controller gains, for turns in the same direction as the gyro rotation, one can find a critical turn rate above which the single gyroscope case will become unstable. This is illustrated in Figure 6, where the single gyro vehicle is stable for a small positive turn rate but unstable for a large positive turn rate. The same two values of turn rate are then simulated for the double gyroscope system, which is stable for both cases (Figure 7).

5   GYROVEHICLE MODEL AND TESTING

A scaled model, shown in Figure 8, has been constructed and is currently being used to test different control strategies. The model is 45cm long, 17cm wide and 20cm high (to the top of the flywheel motor). The model weighs 4.95kg, with the gyroscope's flywheel weighing .75kg, and made out of polished and balanced cold-rolled steel. The flywheel is a cylinder of 7.5cm in diameter and 2.5cm in height. The flywheel is captive in a 6061-T3 frame on a shaft with ball bearings.

The cart has 2cm ground clearance with the current wheel offset (adjustable up to 5cm with 2cm wheel height spacers), and +/- 15 degrees of tilt with stock height (approx +/-30 degrees with 2cm wheel height spacers). The distance from the center of flywheel from the ground-plane is currently 6.5cm (8.5cm with 2cm wheel height spacers). The wheels are 13cm in diameter, with removable traction band. Without the traction band, the wheels will run on 4mm rails (5/32" steel tube or similar).

The tilt sensor is located on-axis located and has an encoder with 1800 counts per rotation (20 counts per degree), and built-in magnetic dampening control. The sensor's bandwidth is 80Hz. The encoder is indexed at 90 degrees to the ground-plane, with a setscrew for zero-trim adjustment.

The tilt and flywheel spin-up motors are Pittman 9413D face mount brush servo motors that run at 18 Volts, DC. The flywheel motor has an encoder integrated with motor for tachometer feedback. The motor drivers are National Semiconductor lmd18201 (Magnevation commercial board). The CPU that runs the control computation is an Atmel AVR Mega128 at 16mhz (via Robostix commercial board). There are two 8.4V batteries. This results in a 16.8V bank at 3000mA-hour (approximately 1 hour runtime on full charge).
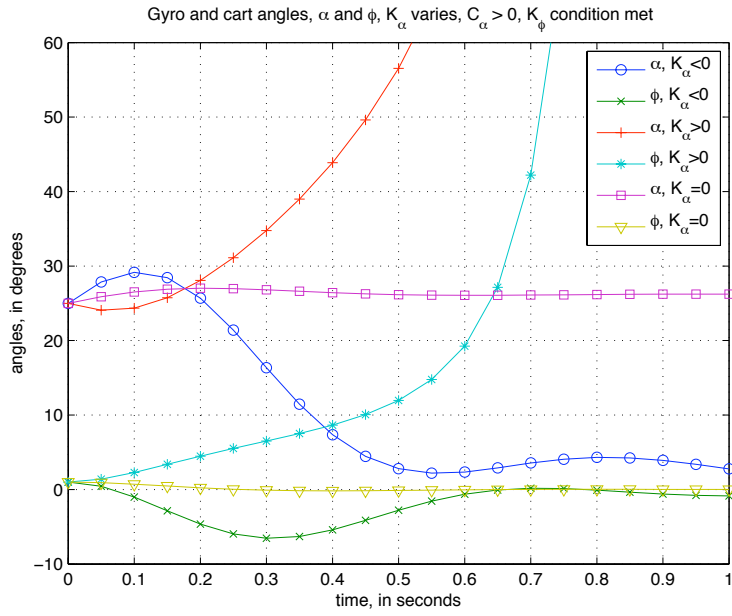
Figure 3: Stability conditions on K_α
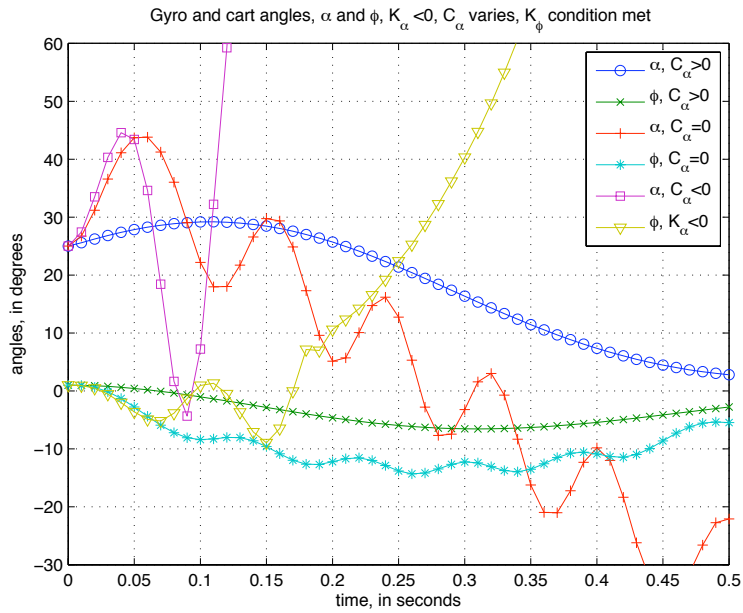
Figure 4: Stability conditions on C_α
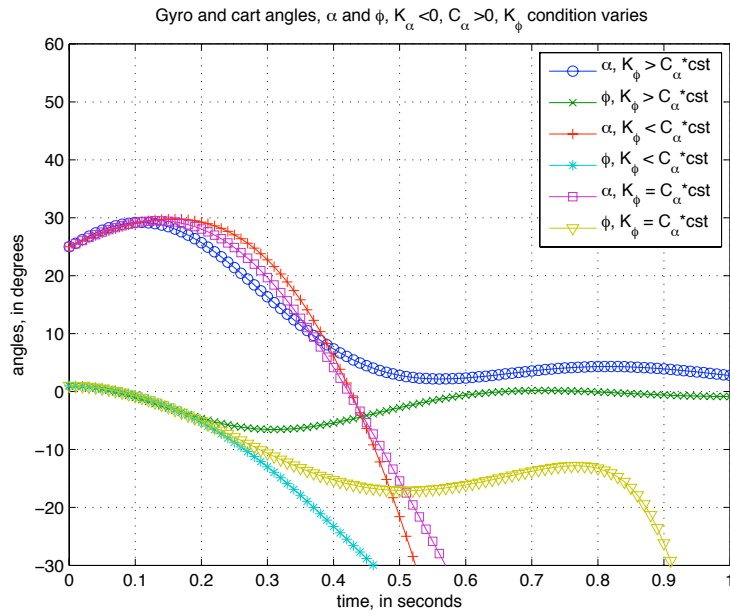
Figure 5: Stability conditions on K_ϕ
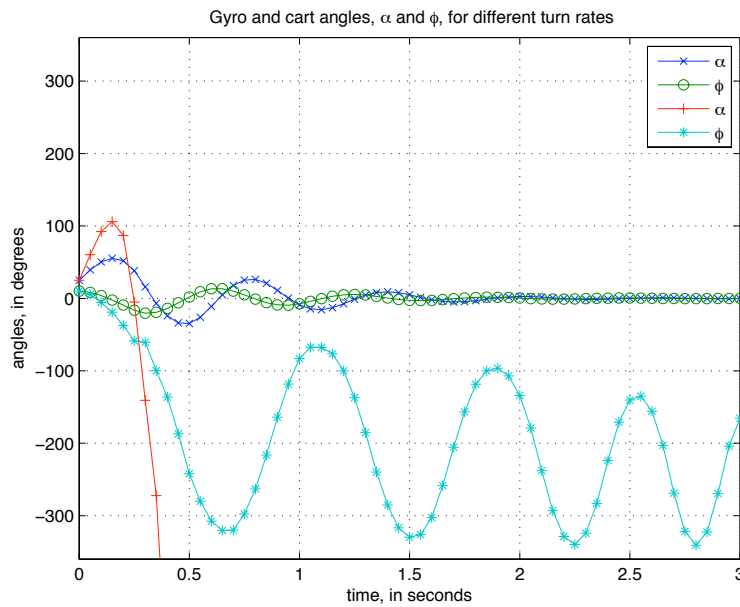
Figure 6: Single gyroscope stability conditions, for different turn rates
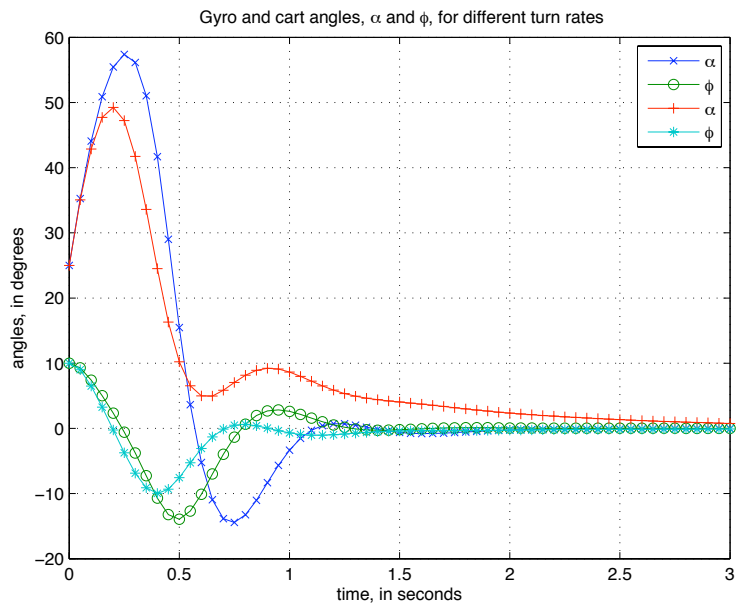
Figure 7: Double gyroscope case, for different turn rates

Figure 8: Gyrovehicle model

6 CONCLUSIONS

We consider the problem of gyropscopic stabilization of unstable vehicles in roll. We derive the full nonlinear equations of motion for the non-trivial case (not just stationary, but straight line motion, curved track, uphill track, unbalanced load, disturbance force) using Lagrangian dynamics, consider different configurations (single and double gyroscope cases), and derive linearized versions of the equations of motion. We consider stability conditions for the linear feedback controller, which yield conditions on controller gains. These conditions were verified in simulation. The stability conditions are dependent on turn rate and direction for the single gyro case, but not for the double gyro case. This is also verified by simulation.

Future work includes further analysis of the equations of motion, and comparisons to other gyroscopic systems such as ship stabilizers. In addition, we will also further analyze control properties, compare the performance of the early mechanical feedback systems to more modern approaches, perform simulations for a full scale vehicle, and analyze results from the scaled model experiments.

7 ACKNOWLEDGMENTS

References

[1] Brennan, L., "Means for Imparting Stability to Unstable Bodies", US Patent No. 796893, 1905

[2] Shilovskii, P.P., "The Gyroscope: its Practical Construction and Application", London, E. and F.N. Spon; New York, Spon and Chamberlain, 1924.

[3] Ferry, E.S., "Applied Gyrodynamics", John Wiley and Sons, Inc, New York, 1933.

[4] Schilowsky, P., "Gyroscope", US Patent No. 1,137,234, 1915.

[5] Samoilescu, G. and Radu, S., "Stabilizers and Stabilizing Systems for Ships", Constantin Brancusi University 8th International Conference, Targu Jiu, May 24-26, 2002.

[6] Adams, J.D. and McKenney, S.W., "Gyroscopic Roll Stabilizer for Boats", US Patent No. 6,973,847, 2005.

[7] http://www.dself.dsl.pipex.com/MUSEUM/museum.htm, The Museum of Retro Technology

[8] Nukulwuthiopas, W., Laowattana, S. and Maneewarn, T., "Dynamic Modeling of a One-Wheel Robot using Kane's Method", Proceedings of the IEEE ICIT 2002 Conference, Bangkok, Thailand, pp. 524-529.

[9] Yabu, A., Okuyama, Y., and Takemori, F., "Attitude Control of Tumbler Systems with One Joint using a Gyroscope", Proceedings of the SICE 1995 Conference, July 26-28, Sapporo, Japan, pp. 1129-1132.

[10] Ahmed, J., Miller, R.H., Hoopman, E.H., Coppola, V.T., Bernstein, D.S., Andrusiak, T. and Acton, D., "An Actively Controlled Moment Gyro/GyroPendulum Testbed", Proceedings of the 1997 IEEE International Conference on Control Applications, Hartford, CT, October 5-7, 1997, pp. 250-252

[11] Beznos, A.V., Formalky, A.M., Gurfinkel, E.V., Jicharev, D.N., Lensky, A.V., Sativsky, K.V. and Tchesalin, L.S., "Control of Autonomous Motion of Two-Wheel Bicycle with Gyroscopic Stabilization", Proceedings of the 1998 IEEE International Conference on Robotics and Automation, Leuven, Belgium, May 1998, pp. 2670-2675.

[12] Gallaspy, J.M., "Gyroscopic Stabilization of an Unmanned Bicycle," M.S. Thesis, Electrical Engineering Department, Auburn University, AL.

[13] Karnopp, D., "Tilt Control for Gyro-Stabilized Two-Wheeled Vehicles", Vehicle System Dynamics, 2002, Vol. 37 No. 2, pp. 145-156.

[14] Cousins, H., "The Stability of Gyroscopic Single Track Vehicles", Engineering, 1913, pp 678-681,711-712,781-784.

[15] Bryson, A. "Control of Spacecraft and Aircraft", Princeton University Press, 1994.